BIOCHEMISTRY
including biophysical chemistry & molecular biology

Article

pubs.acs.org/biochemistry

Using a Fluorescent Cytosine Analogue tC° To Probe the Effect of the Y567 to Ala Substitution on the Preinsertion Steps of dNMP Incorporation by RB69 DNA Polymerase

Shuangluo Xia, Jeff Beckman,† Jimin Wang, and William H. Konigsberg*

Department of Molecular Biophysics and Biochemistry, Yale University, New Haven, Connecticut 06520-8114, United States

ABSTRACT: Residues in the nascent base pair binding pocket (NBP) of bacteriophage RB69 DNA polymerase (RB69pol) are responsible for base discrimination. Replacing Tyr567 with Ala leads to greater flexibility in the NBP, increasing the probability of misincorporation. We used the fluorescent cytosine analogue, 1,3-diaza-2-oxophenoxazine (tC°), to identify preinsertion step(s) altered by NBP flexibility. When tC° is the templating base in a wild-type (wt) RB69pol ternary complex, its fluorescence is quenched only in the presence of dGTP. However, with the RB69pol Y567A mutant, the fluorescence of tC° is also quenched in the presence of dATP. We determined the crystal structure of the dATP/tC°-containing ternary complex of the RB69pol Y567A mutant at 1.9 Å resolution and found that the incoming dATP formed two hydrogen bonds with an imino-tautomerized form of tC°. Stabilization of the dATP/tC° base pair involved movement of the tC° backbone sugar into the DNA minor groove and required tilting of the tC° tricyclic ring to prevent a steric clash with L561. This structure, together with the pre-steady-state kinetic parameters and dNTP binding affinity, estimated from equilibrium fluorescence titrations, suggested that the flexibility of the NBP, provided by the Y567 to Ala substitution, led to a more favorable forward isomerization step resulting in an increase in dNTP binding affinity.

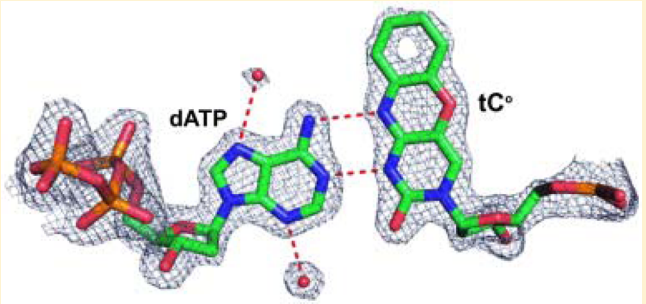

Replication of a genome from any organism must occur with minimal mistakes if the progeny are to remain viable. Replicative DNA polymerases perform this task, making less than one mistake per 10^6 base pairs synthesized.[1−4] Fidelity is increased by an additional 100-fold if the polymerase has exonuclease capability.[5−7] The number of errors made during replication depends on how well a DNA polymerase (pol) can recognize a dNTP as either correct or incorrect for pairing opposite the templating base. Sometimes, a DNA pol can circumvent the geometric constraints imposed by residues in the nascent base pair binding pocket (NBP) so that incorrect dNTPs can be incorporated, albeit with low efficiency.

On the basis of the crystal structures and studies using fluorescent probes, selection of the correct dNTP most likely occurs prior to phosphoryl transfer.[8−16] Subsequent to dNTP binding (Scheme 1), the polymerase Fingers domain closes, aligning the reactive centers of the substrates, leading to rapid nucleotidyl transfer.[13,17−19] The incorrect dNTP either fails to induce Fingers closing, or if the Fingers do close, the result is an unstable, but potentially productive, ternary complex.[13,20,21]

Scheme 1. Pathway of dNTP Binding and Incorporation[a]

$$ED_n + dNTP \underset{k_{-1}}{\overset{k_1}{\rightleftharpoons}} ED_n dNTP \underset{k_{-2}}{\overset{k_2}{\rightleftharpoons}} FD_n dNTP \underset{k_{-3}}{\overset{k_3}{\rightleftharpoons}} FD_{n+1} PPi \xrightarrow{k_4} ED_{n+1} + PPi$$

[a] ED_n is the open complex, and FD_n is the closed complex.

DNA pols from different families, and even within families, differ greatly in their ability to resist insertion of incorrect dNTPs. The B family DNA pol from bacteriophage RB69 (RB69pol) maintains high fidelity even when it encounters damaged templates or templating base analogues.[22−28] Interestingly, upon substitution of Y567 with Ala in the NBP, the mutant RB69pol inserts incorrect dNTPs with efficiencies 10^2−10^3-fold greater than that of wild-type (wt) pol.[29] Crystal structures of ternary complexes of the RB69pol Y567A mutant suggest that the reduction in base selectivity exhibited by this mutant was likely due to an increase in NBP flexibility, leading to stable conformations of the templating base even when it is paired opposite incorrect dNTPs, a situation that would otherwise be blocked in the wt enzyme.[15,29] However, a fuller understanding of how increased flexibility of residues in the NBP affects base selectivity requires analysis of kinetic steps that occur prior to nucleotidyl transfer. For this purpose, we employed the highly fluorescent 1,3-diaza-2-oxophenoxazine (tC°) to probe the preinsertion steps before chemistry. As shown in Figure 1, tC° is a tricyclic cytosine analogue. When present as the templating base, it can be used to follow isomerization of DNA pols from an open to a closed conformation in response to binding of an incoming

Received: February 22, 2012
Revised: April 18, 2012
Published: May 14, 2012

ACS Publications © 2012 American Chemical Society

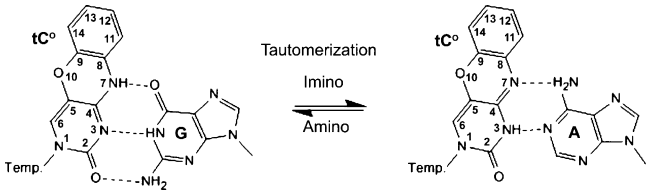

Figure 1. Pairing of guanine (G) and adenine (A) opposite tC°. The analogue pairs with adenine upon tautomerization to the imino form.

dNTP.[12,14] Furthermore, unlike 2-aminopurine (2AP), a well-characterized fluorescent adenine analogue, for which fluorescence quenching is totally dependent on base stacking, quenching of tC° fluorescence depends on the formation of hydrogen bonds (HBs) with the templating base.[30−34] Sandin et al. reported that tC° base pairs exclusively with guanine (G) and causes minimal perturbations in the structure of duplex DNA.[35,36] Kuchta's lab has recently discovered that tC° triphosphate (dtC°TP) is preferentially inserted opposite templating G and A residues by both KF and human DNA pol α.[37] They speculated that the incorporation of dAMP opposite tC° and vice versa was due to the propensity of tC° to tautomerize into its imino form (Figure 1).[37]

We found that the fluorescence of tC° was quenched only when it was paired opposite dGTP in a wt RB69pol ternary complex, reflecting formation of a stable nascent base pair.[15] Surprisingly, we found that the net equilibrium dissociation constant ($K_{d,net}$) for the binding of dGTP opposite tC° with the Y567A mutant, in the absence of chemistry, was reduced by more than 200-fold relative to that of the corresponding wt ternary complex. In addition, dATP was able to form a stable nascent base pair with tC° only with the Y567A mutant. To gain further insight into why this mutant has increased affinity for dGTP and was permissive with respect to dATP binding, we determined the crystal structures of the dGTP/tC° and dATP/tC°-containing ternary complexes of the RB69pol Y567A mutant at 1.9 Å resolution. We found that incoming dATP formed two HBs with an imino-tautomerized form of tC°. However, stabilization of the dATP/tC° base-pair required (i) movement of the tC° backbone sugar into the DNA minor groove; (ii) lateral shifting of residues A567 and G568 toward residue Y416 and; (iii) tilting of the tricyclic ring of tC° base to prevent a steric clash with L561. Together, these data suggest that the flexibility of the NBP provided by replacement of Y567 with Ala led to a more favorable forward isomerization step (higher k_2 value compared to the k_2 exhibited by wt pol, as shown in Scheme 1), resulting in an increase in substrate binding affinity.

EXPERIMENTAL PROCEDURES

Materials. Materials and reagents were of the highest quality commercially available. dNTPs were purchased from Roche (Burgess Hill, U.K.). T4 polynucleotide kinase was purchased from New England Biolabs (Ipswich, MA). [γ-^{32}P]ATP was purchased from MP Biomedicals (Irvine, CA).

Enzymes. Wild-type RB69pol and the Y567A mutant, in an exonuclease-deficient background (D222A and D327A), were overexpressed in *Escherichia coli* strain BL21(DE), purified, and stored as previously described.[38−41]

DNA Substrates. The sequences of the primer/template (P/T) used in this study were 5′-GCGGACTGCTTAC and 5′-TCA(tC°)GTAAGCAGTCCGCG. A dideoxy-terminated primer (ddC at the 3′ end of the primer strand) was used for structural work, fluorescence titrations, and stopped-flow fluorescence experiments. Oligonucleotides were synthesized at the Keck facilities (Yale University). The tC° phosphoramidite was purchased from Glen Research Inc. (Sterling, VA). The primer was labeled at the 5′ end with ^{32}P using T4 polynucleotide kinase and [γ-^{32}P]ATP and annealed to unlabeled templates as previously described.[42,43]

Equilibrium Fluorescence Titrations. Fluorescence emission spectra of 300 nM dideoxy-terminated P/T (tC° at the *n* position of the template strand) with wt or the Y567A mutant (1 μM) and 66 mM Tris-HCl (pH 7.4) and 10 mM $MgSO_4$ were recorded at 23 °C with a Photon Technology International (PTI) scanning spectrofluorometer. We acquired the spectra by exciting the sample at 364 nm and collecting emission from 380 to 700 nm. The intensities were corrected for the intrinsic fluorescence of the enzyme and buffer solutions.

Stopped-Flow Fluorescence Experiments. These experiments were conducted as described previously except that tC° was used in place of 2AP.[14] The excitation and emission wavelengths for tC° were 364 and 450 nm, respectively. The final reaction mixtures consisted of 50 mM Tris (pH7.4), 10 mM $MgCl_2$, 200 nM P/T, 2 μM RB69pol, and varying dGTP concentrations.

Chemical Quench Experiments. Rapid chemical quench experiments were performed at 23 °C with a buffer solution of 66 mM Tris-HCl (pH 7.4) using a Kintek RFQ-3 instrument. For determinations of k_{pol} and $K_{d,app}$, single-turnover conditions were used with a 10-fold excess of RB69pol over P/T. Briefly, enzyme and P/T from one syringe were rapidly mixed with Mg^{2+} and various dNTP concentrations from the other syringe for times ranging from 5 ms to 1 min. The final concentrations after mixing were 1 μM enzyme, 90 nM ^{32}P-labeled P/T, and 10 mM Mg^{2+}. In addition, a 10 × [cold P/T]/[enzyme] ratio was used to ensure that single-turnover conditions were met. Reactions were quenched with 0.5 M EDTA (pH 8.0). Substrates and products were separated by polyacrylamide gel electrophoresis (19:1, w/v, acrylamide−bisacrylamide gels containing 8 M urea), visualized using a STORM imager (Molecular Imaging), and quantitated using Imagequant (GE Healthcare).

Data Analysis. The amount of product formed versus time for each dNTP concentration was fit by nonlinear regression to the single-exponential equation $Y = A[1 - \exp(-k_{obs}t)] + C$ to obtain observed rates of product formation, where Y is the concentration of the DNA product formed during the reaction and C is the offset constant. The kinetic parameters k_{pol} (rate of maximal nucleotide transfer) and $K_{d,app}$ (dNTP concentration at which the rate of phosphoryl transfer reaches $^1/_2k_{pol}$) were obtained by fitting k_{obs} versus dNTP concentration to the hyperbolic equation $k_{obs} = k_{pol}[dNTP]/(K_{d,app} + [dNTP])$, where k_{obs} represents the observed rate at a given dNTP concentration. Note that the $K_{d,app}$ values are not ground-state dissociation constants for dNTP binding. This is because the observed dNTP concentration dependence of the rates of product formation is affected by steps such as the reversible conformational change that occurs subsequent to dNTP binding but prior to phosphoryl transfer.

Crystallization of Y567A RB69pol Ternary Complexes with a dATP/tC° or dGTP/tC° Base Pair. A 13mer dideoxy-terminated primer annealed to a 18mer template strand was used for crystallization. The RB69pol Y567A mutant (final concentration of 120 μM) was mixed with an equimolar ratio of

freshly annealed P/T, and dATP was then added to give a final concentration of 2 mM. Using microbatch vapor-diffusion methods, a solution of 100 mM $CaCl_2$, 15% (w/v) PEG 350 monomethyl ether (MME), and 100 mM sodium cacodylate (pH 6.5) was mixed with an equal volume of the protein complex. Crystals typically grew in 2 days at 20 °C with dimensions of ~100 μm × ~120 μm × ~150 μm. Crystals were transferred from the mother liquor to a cryoprotectant/precipitant stabilization solution containing 20% (w/v) PEG 350 MME, 100 mM $CaCl_2$, and 100 mM sodium cacodylate (pH 6.5) and then to the stabilization solution with the level of PEG 350 increased to 30% (w/v) as a cryoprotectant prior to being frozen in liquid nitrogen.

Data Collection, Structure Determination, and Refinement. X-ray diffraction data were collected using synchrotron radiation sources at beamline 24ID-E of the Northeast Collaborative Access Team (NECAT), Advanced Photon Source (APS), Argonne National Laboratory (ANL), Chicago, IL, at a wavelength of 0.979 Å and 110 K. The crystal belonged to orthorhombic space group $P2_12_12_1$ with different unit cell parameters (Table 1). Data were processed using the HKL2000 program suite.[44]

The structure was determined by molecular replacement using AMORE, starting with the pol structure from the ternary complex of wt RB69pol without the P/T duplex or dNTP,[15] and refined using REFMAC5.[45,46] The P/T duplex and dNTP were built into electron density maps using COOT.[47] Structure refinement statistics are summarized in Table 1. Figures depicting the crystal structures were made using Pymol.[48]

PDB Entries. Coordinates and structure factors for the dATP/tC° and dGTP/tC°-containing ternary complexes of Y567A RB69pol have been deposited in the Protein Data Bank as entries 3QNO and 3QNN, respectively.

Table 1. Crystallographic Statistics for Data Collection and Refinement of the dNTP/tC°-Containing Ternary Complexes of the RB69pol Y567A Mutant[a]

	dATP/tC°	dGTP/tC°
space group	$P2_12_12_1$	$P2_12_12_1$
unit cell dimensions [*a*, *b*, *c* (Å)]	74.9, 120.5, 130.9	74.8, 120.0, 130.0
resolution range (Å)	50.0−1.88	50.0−1.92
no. of unique reflections	90492	85100
redundancy	4.0 (3.2)	4.7 (3.4)
completeness (%)	99.5 (93.8)	99.6 (96.2)
R_{merge}[b] (%)	6.3 (50.7)	10.1 (95.1)
I/σ	18.3 (1.6)	14.4 (1.4)
final model (no.)		
amino acid residues	903	903
water molecules	1001	786
Ca^{2+} ions	4	7
template nucleotides	18	18
primer nucleotides	13	13
dNTP molecules	1	1
Refinement		
no. of reflections	95575	90003
R_{work}[c] (%)	17.4 (26.9)	18.0 (29.8)
R_{free}[d] (%)	21.2 (30.5)	21.3 (34.6)
rmsd[e]		
bond lengths (Å)	0.007	0.008
bond angles (deg)	1.137	1.134
PDB entry	3QNO	3QNN

[a]Statistics for the highest-resolution shell are given in parentheses. [b]$R_{merge} = \sum_{hkl}\sum_j|I_j(hkl) - \langle I(hkl)\rangle|/\sum_{hkl}\sum\langle I(hkl)\rangle$ (statistics for merging all observations for given reflections). [c]$R = \sum_{hkl}|F_{obs}(hkl) - F_{calc}(hkl)|/\sum_{hkl}F_{obs}(hkl)$ (statistics for crystallographic agreement between the measured and model-calculated amplitudes). [d]R_{free} is the agreement for the cross-validation data set. [e]Root mean squares deviations from ideal values.

RESULTS AND DISCUSSION

Incorporation of dGMP and dAMP opposite tC° by wt RB69pol and the Y567A Mutant. Although we had previously shown that the Y567A mutant incorporated incorrect dNMPs more efficiently than wt RB69pol, we were interested in determining how this pol mutant and wt RB69pol would process correct and incorrect incoming dNTPs opposite a templating tC°, a fluorescent analogue of cytosine. Accordingly, we determined the pre-steady-state kinetic parameters for incorporation of dGMP and dAMP opposite tC° by wt RB69pol and the RB69pol Y567A mutant. As shown in Table 2, insertion of dGMP opposite tC° by wt RB69pol was very efficient, with a $k_{pol}/K_{d,app}$ value of 1.8 μM^{-1} s^{-1}, which is comparable to the efficiency of incorporation of dGMP opposite dC (2.9 μM^{-1} s^{-1}), as reported previously.[38] In contrast, the insertion of dAMP opposite tC° by wt RB69pol was 500-fold less efficient than insertion of dGMP, with a $k_{pol}/K_{d,app}$ value of 3.5×10^{-3} μM^{-1} s^{-1} (Table 2 and Figure 2). Via replacement of Y567 with Ala, the efficiency of incorporation of dGMP and dAMP opposite tC° increased 24- and 200-fold, respectively (Table 2 and Figure 2). The 24-fold increase in the efficiency of incorporation of dGMP by the Y567A mutant was mainly due to a 35-fold decrease in $K_{d,app}$ (from 140 μM for wt to 4 μM), while the dramatic increase in the efficiency of incorporation of dAMP by the Y567A mutant was the result of a large increase in k_{pol} (from 6 s^{-1} for wt to 180 s^{-1}) and a large decrease in $K_{d,app}$ (from 1700 μM for wt to 270 μM) (Table 2). In addition, the maximal turnover rates for insertion of dGMP and dAMP opposite tC° by the Y567A mutant were almost identical, in contrast to the 40-fold difference in k_{pol} observed with wt RB69pol.

Table 2. Pre-Steady-State Kinetic Parameters for Incorporation of dAMP and dGMP opposite tC° by wt RB69pol and the Y567A Mutant

RB69pol	dNTP	template	k_{pol} (s^{-1})	$K_{d,app}$ (μM)	$k_{pol}/K_{d,app}$ (μM^{-1} s^{-1})
wt	dATP	tC°	6 ± 0.2	1700 ± 190	3.5×10^{-3}
	dGTP	tC°	250 ± 7	140 ± 18	1.8
Y567A	dATP	tC°	180 ± 10	270 ± 60	0.7
	dGTP	tC°	170 ± 10	4 ± 1	43

Net Binding Affinity of dGMP or dAMP opposite a Templating tC° in a RB69pol Ternary Complex. The value of $K_{d,app}$ determined from our pre-steady-state kinetics experiments was an estimate of the net equilibrium dissociation constant: $K_{d,net} = K_{d,1}/(1 + K_2)$, where $K_{d,1}$ is the ground-state binding constant and K_2 is the equilibrium constant for the isomerization step (ED_ndNTP to FD_ndNTP) according to Scheme 1. Because the fluorescence of tC° is very sensitive to its local environment, we designed a P/T duplex with a dideoxy-terminated ddC at the 3′ end of the primer to measure the net binding affinity of dNTPs opposite tC°. Upon addition of each of the four dNTPs (1 mM) to the wt RB69pol−P/T binary complex, only dGTP quenched the fluorescence of tC°

dx.doi.org/10.1021/bi300241m | Biochemistry 2012, 51, 4609−4617

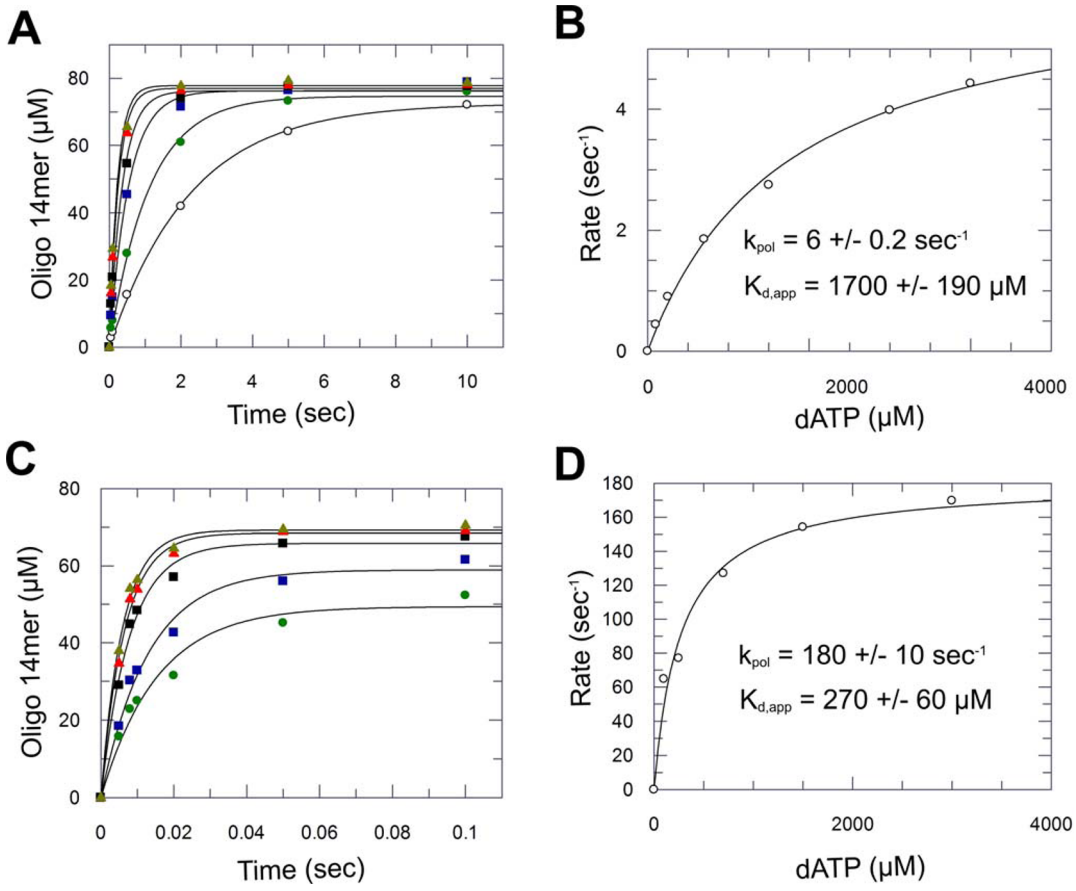

Figure 2. Kinetic insertion of dAMP opposite tC° by wt (A and B) and the Y567A mutant (C and D). (A) Progress curves at 100, 250, 700, 1500, 3000, and 4000 μM dATP (from bottom to top, respectively), fit to a single-exponential equation. (B) Plot of k_{obs} vs [dATP] fit to a hyperbolic equation to yield k_{pol} and $K_{d,app}$. (C) Progress curves at 100, 250, 700, 1500, and 3000 μM dATP (from bottom to top, respectively), fit to a single-exponential equation. (D) Plot of k_{obs} vs [dATP] fit to a hyperbolic equation to yield k_{pol} and $K_{d,app}$.

(by ~30%). In contrast, both dGTP and dATP quenched tC° fluorescence, when added to the Y567A–P/T binary complex (by approximately 30 and 15%, respectively). As shown in Table 3, the $K_{d,net}$ for dGTP with the wt RB69pol–P/T binary complex was 110 μM, which is comparable to the $K_{d,app}$ of 170 μM, determined by single-turnover experiments. Binding of dGTP to the Y567A–P/T binary complex gave a much lower $K_{d,net}$ (0.5 μM), whereas dATP gave a $K_{d,net}$ of 100 μM (Table 3). Thus, substitution of Y567 with Ala decreased the $K_{d,net}$ of dGTP for the pol–P/T binary complex by 220-fold.

Table 3. Fluorescence Titration of dGTP and dATP opposite tC° by wt RB69pol and the Y567A Mutant

RB69pol	dNTP	$K_{d,net}$ (μM)
wt	dGTP	110 ± 27
Y567A	dGTP	0.5 ± 0.2
	dATP	100 ± 40

As an independent check of these results, the $K_{d,net}$ for binding of dGTP to the wt RB69pol–P/T binary complex was estimated using stopped-flow fluorescence. dGTP at various concentrations was rapidly mixed with the wt RB69pol–P/T binary complex, resulting in a series of time courses for tC° fluorescence quenching. When the fluorescence amplitude change was plotted versus dGTP concentration (Figure 3D), a $K_{d,net}$ of 170 μM was obtained, which was comparable to the $K_{d,net}$ value determined by equilibrium fluorescence titration (110 μM). Surprisingly, full quenching of tC° fluorescence occurred within the dead time of the instrument (<2 ms), indicating that the rate of quenching was greater than 500 s^{-1}. This value was at least as fast as the rate of Fingers closing as estimated previously by the rate of 2AP fluorescence quenching.[49]

Crystal Structures of the RB69pol Y567A Mutant in Complex with a Dideoxy P/T Containing a Templating tC° opposite dGTP and dATP. For further insight into how the Y567A mutant was able to insert dGTP or dATP opposite tC° with such high efficiency, we determined two crystal structures of the Y567A mutant in ternary complexes with dGTP/tC° and dATP/tC° nascent base-pairs at 1.92 and 1.88 Å with R_{free} values of 21.3 and 21.2%, respectively (Table 1). Both structures were nearly identical with Cα rmsds (rmsds) of ~0.12 Å. The network of ordered water molecules, particularly those in the vicinity of the NBP, could be clearly visualized because of the high resolution obtained with these crystals. As shown in Figure 4, there are three hydrogen bonds formed between the incoming dGTP and tC°, as expected. In contrast, two hydrogen bonds were observed between the incoming dATP and what is likely to be the imino tautomer of tC°. Otherwise, with the amino tautomer there would be a steric clash between the N6-H group of adenine and the N7-H group of the amino tautomer of tC° as the interatomic distance between the two nitrogen atoms is 3.1 Å. The interatomic distance between N1 of adenine and N3 of tC° was 2.7 Å. This

dx.doi.org/10.1021/bi300241m | *Biochemistry* 2012, 51, 4609–4617

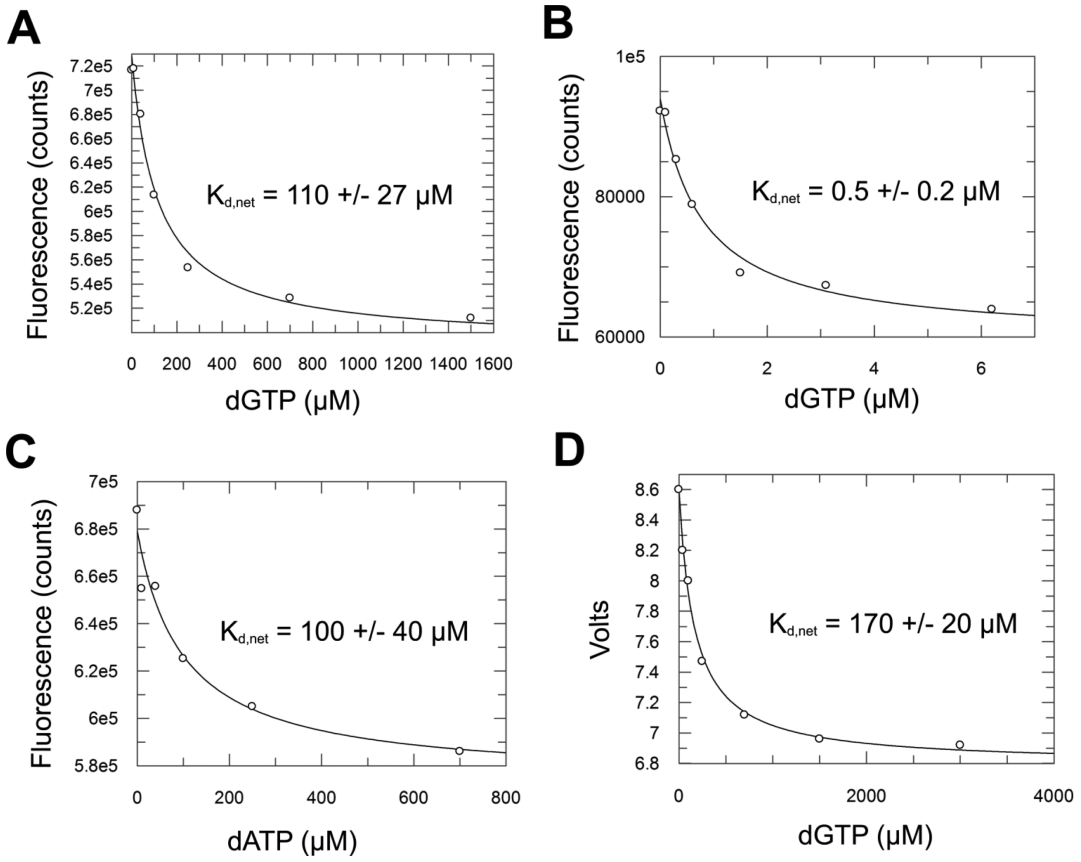

Figure 3. Results of fluorescence titrations of dNTPs opposite tC° in P/T complexes with wt and the Y567A mutant. Dissociation constants ($K_{d,net}$) for (A) binding of dGTP opposite tC° in the wt ternary complex, (B) binding of dGTP opposite tC° in the Y567A mutant ternary complex, and (C) binding of dATP opposite tC° in the Y567A mutant ternary complex. (D) Plot of changes in amplitude obtained by stopped-flow fluorescence for dGTP opposite tC° with wt RB69pol.

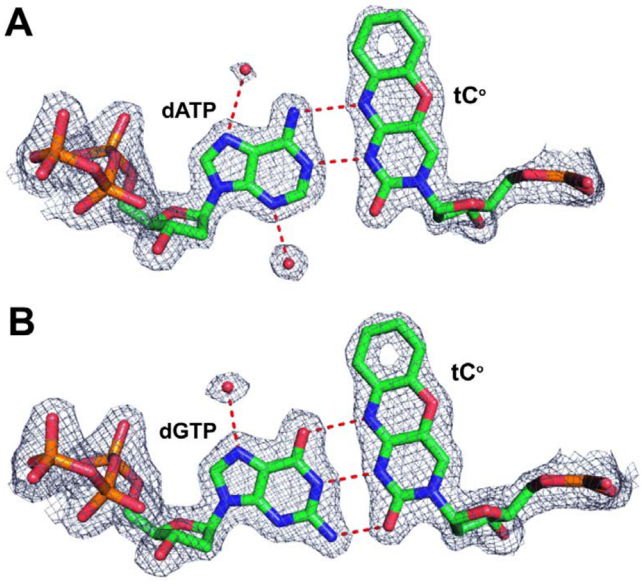

Figure 4. Structures of dNTP/tC° nascent base pairs in the ternary complexes of the RB69pol Y567A mutant. (A) Final $2F_o - F_c$ electron desnity map at 1.88 Å resolution for the dATP/tC°-containing complex contoured at 1.8σ. (B) Final $2F_o - F_c$ electron density map at 1.92 Å resolution for the dGTP/tC°-containing complex contoured at 1.8σ.

observation is consistent with the prediction by Kuchta et al.[37] that the imino tautomer of tC° and adenine presumably forms a base pair that is isosteric with a dT/dA base pair.

Via superimposition of the palm domains of the structure of the dATP/tC°-containing Y567A RB69pol ternary complex with that of the 1.8 Å resolution structure of the dCTP/dG-containing wt ternary complex,[15] it appeared that the A567 and G568 residues in the Y567A mutant shifted laterally toward the Y416 side chain and vertically into the DNA minor groove by approximately 0.7 and 0.4 Å, respectively, compared to their positions in the wt structure (Figure 5A). In addition, the sugar moiety of the templating tC° shifted by a similar distance so that interactions between G568 and tC° in the Y567A mutant are similar to those between G568 and the templating dC in the wt enzyme (Figure 5A). Presumably, the movement of the sugar backbone into the space provided by the shifting of residues A567 and G568 prevented a potential steric clash of the tC° tricyclic ring with the side chain of L561 (Figure 6A). However, this movement caused the tC° base to tilt slightly toward the penultimate base pair at the P/T junction creating a slight twist in the dATP/tC° nascent base-pair geometry (Figure 6A). Also, the O2 of tC° overlays nicely with N3 of guanine when paired with an incoming dCTP mimicking Watson–Crick-like geometry. When the dGTP/tC°-containing Y567A mutant structure was superimposed on the dCTP/dG-containing wt structure, similar shifts of A567 and G568 were observed (Figure 5B). Again, the tricyclic ring of tC° tilted toward the duplex DNA, preventing a clash with the side chain

dx.doi.org/10.1021/bi300241m | *Biochemistry* 2012, 51, 4609–4617

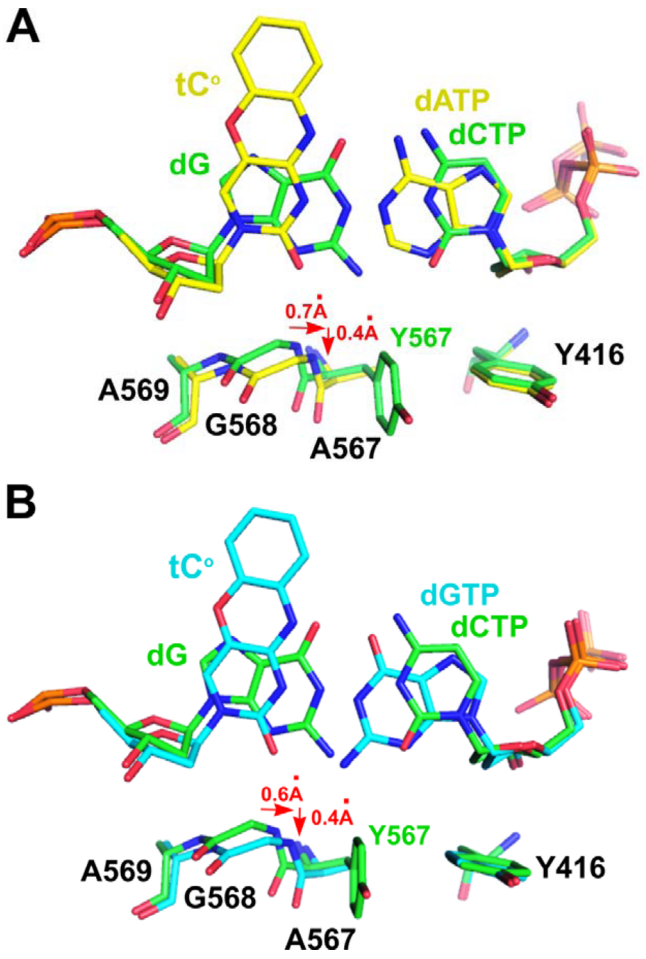

Figure 5. (A) Superposition of the dATP/tC°-containing Y567A mutant ternary complex (yellow) with the dCTP/dG-containing wt ternary complex (green). (B) Superposition of the dGTP/tC°-containing Y567A mutant ternary complex (cyan) with the dCTP/dG-containing wt ternary complex (green).

of L561 (Figure 6B). The downward movement of the sugar moiety of the templating tC° and the lateral shift of residues A567 and G568 cannot occur in wt RB69pol because of the rigidity of the NBP. This could explain why the efficiency of

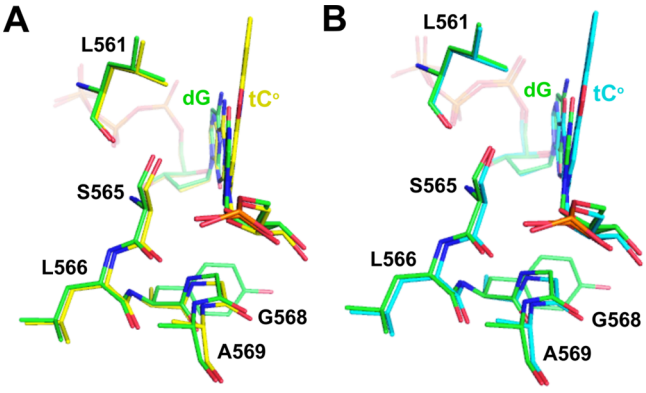

Figure 6. (A) Superposition of the dATP/tC°-containing Y567A mutant ternary complex (yellow) with the dCTP/dG-containing wt ternary complex (green). (B) Superposition of the dGTP/tC°-containing Y567A mutant ternary complex (cyan) with the dCTP/dG-containing wt ternary complex (green).

incorporation of dGMP and dAMP opposite tC° increased dramatically upon substitution of Y567 with Ala.

In the structure of the dATP/tC°-containing Y567A RB69pol ternary complex, there are two alternative conformations of the 5′ template strand overhang (Figure 7). In one conformation,

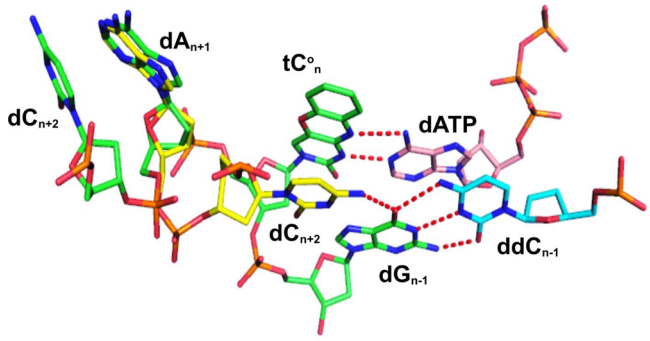

Figure 7. Two alternative conformations of the 5′ overhang of the template strand in the dATP/tC°-containing Y567A mutant ternary complex. The template strand is colored green. The overhanging DNA in the alternative conformation is colored yellow.

the base of dC at position $n + 2$ of the template strand was stacked on top of the dA base at position $n + 1$ in the template. In the other conformation, dC at position $n + 2$ of the template was flipped back into the NBP, forming a Hoogsteen base pair with dG at position $n - 1$ of the template strand (Figure 7). This backward flip of dC at position $n + 2$ of the template was also stabilized by $\pi-\pi$ interactions between tC° and the base of dC at position $n + 2$ (Figure 7). The occupancy of this alternative conformation of the 5′ template overhang in the dGTP/tC°-containing Y567A ternary complex was much lower than in the dATP/tC°-containing Y567A ternary complex so that it was nearly unobservable.

Tautomerization of tC° in the Y567A Mutant Ternary Complex. Our structural data suggest that a potential steric clash would occur between L561 and tC° that could cause the dATP/tC° nascent base-pair in the wt RB69pol ternary complex to be rejected if the side chain of L561 cannot adopt an alternative rotamer conformation. Another possible interpretation of the kinetic behavior of wt RB69pol, with respect to the insertion of dAMP opposite tC°, is that the rigidity of the NBP of wt RB69pol prevents tautomerization of tC° within the ternary complex. It has been reported that unmodified cytosine exists mainly as the amino tautomer in solution with an estimated amino:imino ratio of 10,000:1.[37] Thus, it is likely that the amino tautomeric form of tC° is more highly populated than the imino form both in solution and presumably within the initial collision complex. Upon formation of the closed ternary complex, interactions between the enzyme and the dATP/tC° base-pair stabilize the imino form of tC°, shifting the equilibrium toward the imino form. Because of the flexibility of the NBP in the Y567A mutant, the amino to imino conversion occurs within the closed ternary complex so that the imino form of tC° is captured. In contrast, for wt RB69pol, the rigidity of the NPB creates a much higher energy barrier for this conversion so that it is unlikely to occur. The resulting amino tautomer of the tC°/dATP wobble base pair causes a steric clash with Y567 and L561 of the NBP with wt RB69pol and would be rejected from the ternary complex. Possibly, the prevention of the amino to imino conversion by

dx.doi.org/10.1021/bi300241m | *Biochemistry* 2012, 51, 4609−4617

wt RB69pol could be a general mechanism for rejecting minor tautomers of mispaired bases.

Increased Flexibility of the NBP Leads to a More Favorable Forward Isomerization Step. Previous work by several groups, using fluorescent probes attached to the DNA pol or as fluorescent DNA bases, has shown that selection of dNTPs by DNA pols, including those from T7, Klentaq, KF, T4, and RB69, likely occurs prior to or during formation of the closed ternary complex.[10,13,14,22,50,51] Our stopped-flow fluorescence experiments showed that binding of dGTP opposite tC° in the NBP of wt or the Y567A RB69pol mutant led to very rapid quenching of tC° fluorescence (>500 s^{-1}). This suggested that the formation of a stable dGTP/tC° nascent base pair, including proper alignment of reactive groups and catalytic residues, occurs concomitantly with the Fingers domain closing into a closed, preinsertion complex. Both pre-steady-state kinetic experiments and fluorescence titration experiments show that $K_{d,app}$ and $K_{d,net}$ for both dGTP and dATP decrease dramatically upon replacement of Y567 with Ala. According to Scheme 1, $K_{d,net}$ is defined as $K_{d,1}/(1 + K_2)$. It is unlikely that the Y567A mutation would influence formation of the initial collision complex ($K_{d,1}$). Therefore, a more favorable forward commitment must be controlled by K_2 with the mutant enzyme. This could be due to a more rapid forward rate constant (k_2) relative to that of the wt enzyme because of the increased NBP flexibility resulting from the Y567 to Ala substitution. This notion is supported by our structural data showing that a downward movement of the sugar moiety of the templating tC° and the lateral shifting of residues A567 and G568 occurred with the Y567A mutant but not with wt RB69pol. It is also consistent with our previously reported structures of dCTP/dG-containing ternary complexes of wt RB69pol and Y567A mutant that showed that an inter-residue HB between Y567 and Y391 is responsible for helix P and residue G568 being in a strained geometry.[15] By disruption of this HB interaction by the Y567 to Ala substituion, G568 was able to relax into a new position with both the dCTP/dG and dTTP/dG base-pairs. Our observations provide an example of how an increase in substrate binding affinity can result from an increase in k_2.

tC° Can Potentially Be Used as a Probe for Monitoring Conformational Changes in Other DNA pols. Because the NBPs of all B family replicative pols contain highly conserved residues,[52] including a Tyr at a position analogous to position 567 in RB69pol, we propose that this correlation between rigidity and base selectivity is likely to be generally applicable to pols in the B family. Thus, it appears that tC° is a useful templating base analogue for testing the effect of amino acid substitutions on NBP flexibility in other B family pols, because it detects the formation of stable nascent base pairs. In addition, tC° can also be used to determine kinetic parameters of preinsertion steps within the catalytic cycle. However, its potential was limited in the case of RB69pol, because the forward rate constants for formation of a closed ternary complex are too large to determine accurately using our stopped-flow fluorescence instrument. Some replicative DNA pols, such as T7 DNA pol,[13] isomerize to the active ternary complex more slowly and therefore are able to provide the desired data for the rates of closing of the Fingers domain.

In summary, increasing the flexibility of amino acid residues on the DNA minor groove side of the NBP in the Y567A mutant leads to highly efficient insertion of incorrect dNTPs. Data provided by analysis of tC° fluorescence quenching and crystal structures reveal that the increased flexibility provided by the Y567A mutant has the effect of increasing the stability of the ternary complex following the preinsertion isomerization step by helping tC° avoid a steric clash with L561 as it shifts down toward the templating tC° base to form a closed ternary complex. Finally, the data also show that L561 in wt RB69pol is rigid, along with G568 and A569, and that these three residues form a network that prevents unnaturally large templating base analogues from forming stable interactions with incoming dNTPs.

AUTHOR INFORMATION

Corresponding Author

*SHM CE-14, Department of Molecular Biophysics and Biochemistry, Yale University, New Haven, CT 06520-8114. Telephone: (203) 785-4599. Fax: (203) 785-7979. E-mail: william.konigsberg@yale.edu.

Present Address

[†]Genzyme Corp., Cambridge, MA 02142.

Author Contributions

S.X. and J.B. contributed equally to this work.

Funding

This work was supported by National Institutes of Health Grants RO1-GM063276-09 (to W.H.K.) and by SCSB-GIST (to J.W.).

Notes

The authors declare no competing financial interest.

ACKNOWLEDGMENTS

We thank the staff of NE-CAT beamline 24-ID-E at the Advanced Photon Source of Argonne National Laboratory.

ABBREVIATIONS

pol, polymerase; exo, exonuclease; RB69pol, RB69 DNA polymerase; NBP, nascent base pair binding pocket; P/T, primer/template; W−C, Watson−Crick; wt, wild type; HB, hydrogen bond or hydrogen bonding; KF, Klenow fragment; tC°, 1,3-diaza-2 oxophenoxazine; 2AP, 2-aminopurine; $K_{d,net}$, $K_{d,1}/(1 + K_2)$ without chemistry; $K_{d,app}$, dNTP concentration that gives a k_{obs} that is half the maximal rate, k_{pol}; $K_{d,1}$, k_{-1}/k_1; K_2, k_2/k_{-2}; PDB, Protein Data Bank.

REFERENCES

(1) Drake, J. W. (1969) Comparative rates of spontaneous mutation. *Nature 221*, 1132.

(2) Echols, H., and Goodman, M. F. (1991) Fidelity mechanisms in DNA replication. *Annu. Rev. Biochem. 60*, 477−511.

(3) Kunkel, T. A., and Bebenek, K. (2000) DNA replication fidelity. *Annu. Rev. Biochem. 69*, 497−529.

(4) Kunkel, T. A. (2004) DNA replication fidelity. *J. Biol. Chem. 279*, 16895−16898.

(5) Brutlag, D., and Kornberg, A. (1972) Enzymatic synthesis of deoxyribonucleic acid. 36. A proofreading function for the 3′ leads to 5′ exonuclease activity in deoxyribonucleic acid polymerases. *J. Biol. Chem. 247*, 241−248.

(6) Muzyczka, N., Poland, R. L., and Bessman, M. J. (1972) Studies on the biochemical basis of spontaneous mutation. I. A comparison of the deoxyribonucleic acid polymerases of mutator, antimutator, and wild type strains of bacteriophage T4. *J. Biol. Chem. 247*, 7116−7122.

(7) Kunkel, T. A. (1988) Exonucleolytic proofreading. *Cell 53*, 837−840.

(8) Capson, T. L., Peliska, J. A., Kaboord, B. F., Frey, M. W., Lively, C., Dahlberg, M., and Benkovic, S. J. (1992) Kinetic characterization of

the polymerase and exonuclease activities of the gene 43 protein of bacteriophage T4. *Biochemistry 31*, 10984−10994.
(9) Franklin, M. C., Wang, J., and Steitz, T. A. (2001) Structure of the replicating complex of a pol α family DNA polymerase. *Cell 105*, 657−667.
(10) Purohit, V., Grindley, N. D., and Joyce, C. M. (2003) Use of 2-aminopurine fluorescence to examine conformational changes during nucleotide incorporation by DNA polymerase I (Klenow fragment). *Biochemistry 42*, 10200−10211.
(11) Hariharan, C., and Reha-Krantz, L. J. (2005) Using 2-aminopurine fluorescence to detect bacteriophage T4 DNA polymerase-DNA complexes that are important for primer extension and proofreading reactions. *Biochemistry 44*, 15674−15684.
(12) Hariharan, C., Bloom, L. B., Helquist, S. A., Kool, E. T., and Reha-Krantz, L. J. (2006) Dynamics of nucleotide incorporation: Snapshots revealed by 2-aminopurine fluorescence studies. *Biochemistry 45*, 2836−2844.
(13) Tsai, Y. C., and Johnson, K. A. (2006) A new paradigm for DNA polymerase specificity. *Biochemistry 45*, 9675−9687.
(14) Zhang, H., Cao, W., Zakharova, E., Konigsberg, W., and De La Cruz, E. M. (2007) Fluorescence of 2-aminopurine reveals rapid conformational changes in the RB69 DNA polymerase-primer/template complexes upon binding and incorporation of matched deoxynucleoside triphosphates. *Nucleic Acids Res. 35*, 6052−6062.
(15) Wang, M., Xia, S., Blaha, G., Steitz, T. A., Konigsberg, W. H., and Wang, J. (2011) Insights into base selectivity from the 1.8 Å resolution structure of an RB69 DNA polymerase ternary complex. *Biochemistry 50*, 581−590.
(16) Xia, S., Wang, M., Blaha, G., Konigsberg, W. H., and Wang, J. (2011) Structural Insights into Complete Metal Ion Coordination from Ternary Complexes of B Family RB69 DNA Polymerase. *Biochemistry 50*, 9114−9124.
(17) Joyce, C. M., and Steitz, T. A. (1994) Function and structure relationships in DNA polymerases. *Annu. Rev. Biochem. 63*, 777−822.
(18) Joyce, C. M., and Benkovic, S. J. (2004) DNA polymerase fidelity: Kinetics, structure, and checkpoints. *Biochemistry 43*, 14317−14324.
(19) Bakhtina, M., Roettger, M. P., Kumar, S., and Tsai, M. D. (2007) A unified kinetic mechanism applicable to multiple DNA polymerases. *Biochemistry 46*, 5463−5472.
(20) Johnson, K. A. (2008) Role of induced fit in enzyme specificity: A molecular forward/reverse switch. *J. Biol. Chem. 283*, 26297−26301.
(21) Johnson, K. A. (2010) The kinetic and chemical mechanism of high-fidelity DNA polymerases. *Biochim. Biophys. Acta 1804*, 1041−1048.
(22) Frey, M. W., Sowers, L. C., Millar, D. P., and Benkovic, S. J. (1995) The nucleotide analog 2-aminopurine as a spectroscopic probe of nucleotide incorporation by the Klenow fragment of *Escherichia coli* polymerase I and bacteriophage T4 DNA polymerase. *Biochemistry 34*, 9185−9192.
(23) Fidalgo da Silva, E., Mandal, S. S., and Reha-Krantz, L. J. (2002) Using 2-aminopurine fluorescence to measure incorporation of incorrect nucleotides by wild type and mutant bacteriophage T4 DNA polymerases. *J. Biol. Chem. 277*, 40640−40649.
(24) Mandal, S. S., Fidalgo da Silva, E., and Reha-Krantz, L. J. (2002) Using 2-aminopurine fluorescence to detect base unstacking in the template strand during nucleotide incorporation by the bacteriophage T4 DNA polymerase. *Biochemistry 41*, 4399−4406.
(25) Beckman, J., Wang, M., Blaha, G., Wang, J., and Konigsberg, W. H. (2010) Substitution of Ala for Tyr567 in RB69 DNA polymerase allows dAMP to be inserted opposite 7,8-dihydro-8-oxoguanine. *Biochemistry 49*, 4116−4125.
(26) Beckman, J., Wang, M., Blaha, G., Wang, J., and Konigsberg, W. H. (2010) Substitution of Ala for Tyr567 in RB69 DNA polymerase allows dAMP and dGMP to be inserted opposite guanidino hydantoin. *Biochemistry 49*, 8554−8563.
(27) Xia, S., Konigsberg, W. H., and Wang, J. (2011) Hydrogen-bonding capability of a templating difluorotoluene nucleotide residue in an RB69 DNA polymerase ternary complex. *J. Am. Chem. Soc. 133*, 10003−10005.
(28) Xia, S., Eom, S. H., Konigsberg, W. H., and Wang, J. (2012) Structural Basis for Differential Insertion Kinetics of dNMPs Opposite a Difluorotoluene Nucleotide Residue. *Biochemistry 51*, 1476−1485.
(29) Reha-Krantz, L. J., Hariharan, C., Subuddhi, U., Xia, S., Zhao, C., Beckman, J., Christian, T., and Konigsberg, W. (2011) Structure of the 2-aminopurine-cytosine base pair formed in the polymerase active site of the RB69 Y567A-DNA polymerase. *Biochemistry 50*, 10136−10149.
(30) Engman, K. C., Sandin, P., Osborne, S., Brown, T., Billeter, M., Lincoln, P., Norden, B., Albinsson, B., and Wilhelmsson, L. M. (2004) DNA adopts normal B-form upon incorporation of highly fluorescent DNA base analogue tC: NMR structure and UV-Vis spectroscopy characterization. *Nucleic Acids Res. 32*, 5087−5095.
(31) Stengel, G., Gill, J. P., Sandin, P., Wilhelmsson, L. M., Albinsson, B., Norden, B., and Millar, D. (2007) Conformational dynamics of DNA polymerase probed with a novel fluorescent DNA base analogue. *Biochemistry 46*, 12289−12297.
(32) Magat Juan, E. C., Shimizu, S., Ma, X., Kurose, T., Haraguchi, T., Zhang, F., Tsunoda, M., Ohkubo, A., Sekine, M., Shibata, T., Millington, C. L., Williams, D. M., and Takenaka, A. (2010) Insights into the DNA stabilizing contributions of a bicyclic cytosine analogue: Crystal structures of DNA duplexes containing 7,8-dihydropyrido [2,3-d]pyrimidin-2-one. *Nucleic Acids Res. 38*, 6737−6745.
(33) Preus, S., Borjesson, K., Kilsa, K., Albinsson, B., and Wilhelmsson, L. M. (2010) Characterization of nucleobase analogue FRET acceptor tCnitro. *J. Phys. Chem. B 114*, 1050−1056.
(34) Wilhelmsson, L. M. (2010) Fluorescent nucleic acid base analogues. *Q. Rev. Biophys. 43*, 159−183.
(35) Sandin, P., Wilhelmsson, L. M., Lincoln, P., Powers, V. E., Brown, T., and Albinsson, B. (2005) Fluorescent properties of DNA base analogue tC upon incorporation into DNA: Negligible influence of neighbouring bases on fluorescence quantum yield. *Nucleic Acids Res. 33*, 5019−5025.
(36) Sandin, P., Borjesson, K., Li, H., Martensson, J., Brown, T., Wilhelmsson, L. M., and Albinsson, B. (2008) Characterization and use of an unprecedentedly bright and structurally non-perturbing fluorescent DNA base analogue. *Nucleic Acids Res. 36*, 157−167.
(37) Stengel, G., Purse, B. W., Wilhelmsson, L. M., Urban, M., and Kuchta, R. D. (2009) Ambivalent incorporation of the fluorescent cytosine analogues tC and tCo by human DNA polymerase α and Klenow fragment. *Biochemistry 48*, 7547−7555.
(38) Zhang, H., Beckman, J., Wang, J., and Konigsberg, W. (2009) RB69 DNA polymerase mutants with expanded nascent base-pair-binding pockets are highly efficient but have reduced base selectivity. *Biochemistry 48*, 6940−6950.
(39) Xia, S., Wang, M., Lee, H. R., Sinha, A., Blaha, G., Christian, T., Wang, J., and Konigsberg, W. (2011) Variation in mutation rates caused by RB69pol fidelity mutants can be rationalized on the basis of their kinetic behavior and crystal structures. *J. Mol. Biol. 406*, 558−570.
(40) Xia, S., Eom, S. H., Konigsberg, W. H., and Wang, J. (2012) Bidentate and tridentate metal-ion coordination states within ternary complexes of RB69 DNA polymerase. *Protein Sci. 21*, 447−451.
(41) Zhang, H., Rhee, C., Bebenek, A., Drake, J. W., Wang, J., and Konigsberg, W. (2006) The L561A substitution in the nascent base-pair binding pocket of RB69 DNA polymerase reduces base discrimination. *Biochemistry 45*, 2211−2220.
(42) Maniatis, T., Fritsch, E. F., and Sambrook, J., Eds. (1982) *Molecular cloning: A laboratory nanual*, Cold Spring Harbor Laboratory Press, Plainview, NY.
(43) Kuchta, R. D., Mizrahi, V., Benkovic, P. A., Johnson, K. A., and Benkovic, S. J. (1987) Kinetic mechanism of DNA polymerase I (Klenow). *Biochemistry 26*, 8410−8417.
(44) Otwinowski, Z., and Minor, W. (1997) Processing of X-ray diffraction data collected in oscillation mode. In *Methods in Enzymology* (Carter, C. W., and Sweet, R. M., Eds.) pp 307−326, Elsevier, Amsterdam.

(45) Murshudov, G. N., Vagin, A. A., and Dodson, E. J. (1997) Refinement of macromolecular structures by the maximum-likelihood method. *Acta Crystallogr. D53*, 240−255.
(46) Navaza, J. (1994) AMoRe: an automated package for molecular replacement. *Acta Crystallogr. A50*, 157−163.
(47) Emsley, P., and Cowtan, K. (2004) Coot: Model-building tools for molecular graphics. *Acta Crystallogr. D60*, 2126−2132.
(48) *The PyMOL Molecular Graphics System*, version 1.2r3pre (2010) Schrodinger, LLC, New York.
(49) Lee, H. R., Wang, M., and Konigsberg, W. (2009) The reopening rate of the fingers domain is a determinant of base selectivity for RB69 DNA polymerase. *Biochemistry 48*, 2087−2098.
(50) Rothwell, P. J., Mitaksov, V., and Waksman, G. (2005) Motions of the fingers subdomain of Klentaq1 are fast and not rate limiting: Implications for the molecular basis of fidelity in DNA polymerases. *Mol. Cell 19*, 345−355.
(51) Christian, T. D., Romano, L. J., and Rueda, D. (2009) Single-molecule measurements of synthesis by DNA polymerase with base-pair resolution. *Proc. Natl. Acad. Sci. U.S.A. 106*, 21109−21114.
(52) Braithwaite, D. K., and Ito, J. (1993) Compilation, alignment, and phylogenetic relationships of DNA polymerases. *Nucleic Acids Res. 21*, 787−802.